Biophysical Journal, Volume *120*

Supplemental Information

Mechanisms of Premature Ventricular Complexes Caused by QT Prolongation

Zhaoyang Zhang, Michael B. Liu, Xiaodong Huang, Zhen Song, and Zhilin Qu

Supplemental Information

Table S1. **Maximum conductance of ionic currents in the AP models**. Listed are the maximum conductance of the major ionic currents from the original models. The units as the same as in the original AP models.

	G_{Na}	P_{Ca}	G_{Ks}	G_{Kr}	G_{to} ($G_{to,f}$)	$G_{to,s}$	G_{K1}	v_{NCX}
LRd	16.0	5.4×10^{-4}	0.433	0.02614	0.50	/	0.75	0.00025
SB	16.0	5.4×10^{-4}	0.07	0.03	0.02	0.06	0.9	9.0
HRd	8.25	2.43×10^{-4}	0.0248975	0.0138542	0.19	/	0.50	4.5
TP04	14.838	1.75×10^{-4}	0.245	0.096	0.294	/	5.405	1000.0
GB	23.0	1.25×10^{-4}	0.0035	0.035	0.1144	0.0156	0.35	4.5
ORd	16.0	1×10^{-4}	0.0034	0.046	0.02	/	0.1908	0.0008
ToRORd	11.7802	8.3757×10^{-5}	0.0011	0.0321	0.16	/	0.6992	0.0034

Table S2. **The parameter intervals for the randomly drawn parameters**. $\alpha(P_{Ca})$ is in the same range as in Fig.1 and Fig.2 in the main text. $\beta(G_{Ks})$ is a random number between 0.5 and 2 times the value used in Fig.2 for LQT2 of each model. $\alpha(G_{Ks})$ is a random number between 0 and 1 times $\beta(G_{Ks})$. In other words, in each simulation, a $\beta(G_{Ks})$ value was first drawn randomly from the assigned interval, and then this $\beta(G_{Ks})$ value was multiplied by a random number between 0 and 1 to give rise to the $\alpha(G_{Ks})$ value.

	$\alpha(P_{Ca})$	$\beta(G_{Ks})$	$\alpha(G_{Ks})$	$\alpha(G_{Kr})$	$\alpha(G_{to,f})$	$\alpha(G_{to,s})$	$\alpha(G_{K1})$	$\alpha(v_{NCX})$	$\alpha(G_{NaL})$
LRd	[0, 5]	[0.5, 2]*2	$\beta(G_{Ks})$*[0, 1]	[0, 2]	[0, 2]	/	[0.5, 2]	[0.5, 2]	[0, 10]
SB	[0, 6]	[0.5, 2]*10	$\beta(G_{Ks})$*[0, 1]	[0, 2]	[0, 2]	[0, 2]	[0.5, 2]	[0.5, 2]	[0, 10]
TP04	[0, 20]	[0.5, 2]*2	$\beta(G_{Ks})$*[0, 1]	[0, 2]	[0, 2]	/	[0.5, 2]	[0.5, 2]	[0, 10]
GB	[0, 6]	[0.5, 2]*30	$\beta(G_{Ks})$*[0, 1]	[0, 2]	[0, 2]	[0, 2]	[0.5, 2]	[0.5, 2]	[0, 10]
ORd	[0, 15]	[0.5, 2]*10	$\beta(G_{Ks})$*[0, 1]	[0, 2]	[0, 2]	/	[0.5, 2]	[0.5, 2]	[0, 10]
ToRORd	[0, 6]	[0.5, 2]*20	$\beta(G_{Ks})$*[0, 1]	[0, 2]	[0, 2]	/	[0.5, 2]	[0.5, 2]	[0, 10]

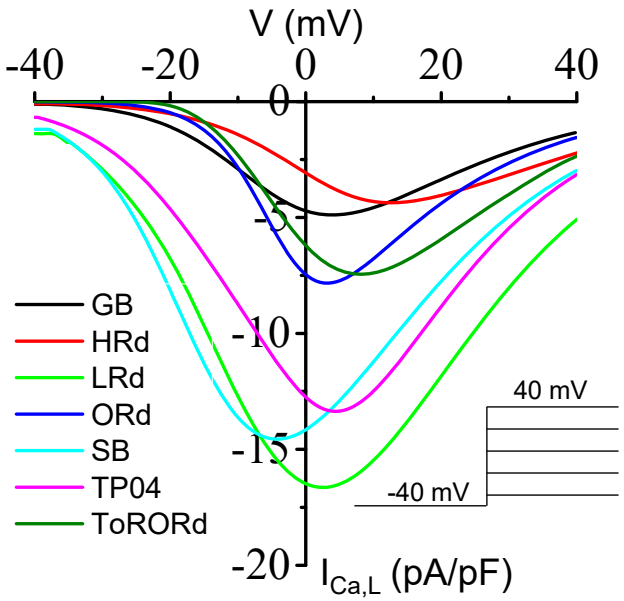

Figure S1. **I-V curves for $I_{Ca,L}$ of the AP models**. Peak $I_{Ca,L}$ versus test potentials obtained under a voltage-clamp protocol as indicated.

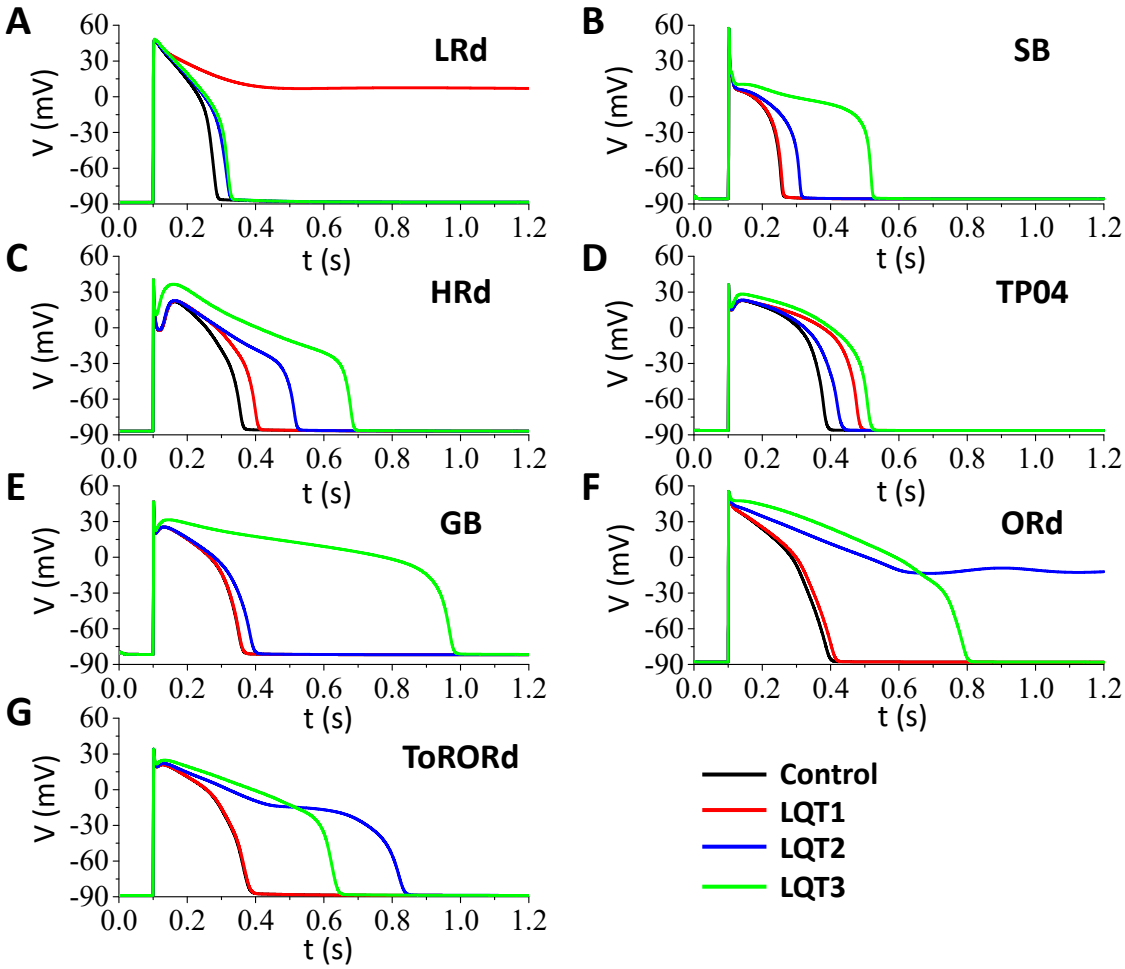

Figure S2. **APs under normal control and the conditions of LQT1, LQT2, and LQT3**. **A**. LRd. **B**. SB. **C**. HRd. **D**. TP04. **E**. GB. **F**. ORd. **G**. ToRORd.

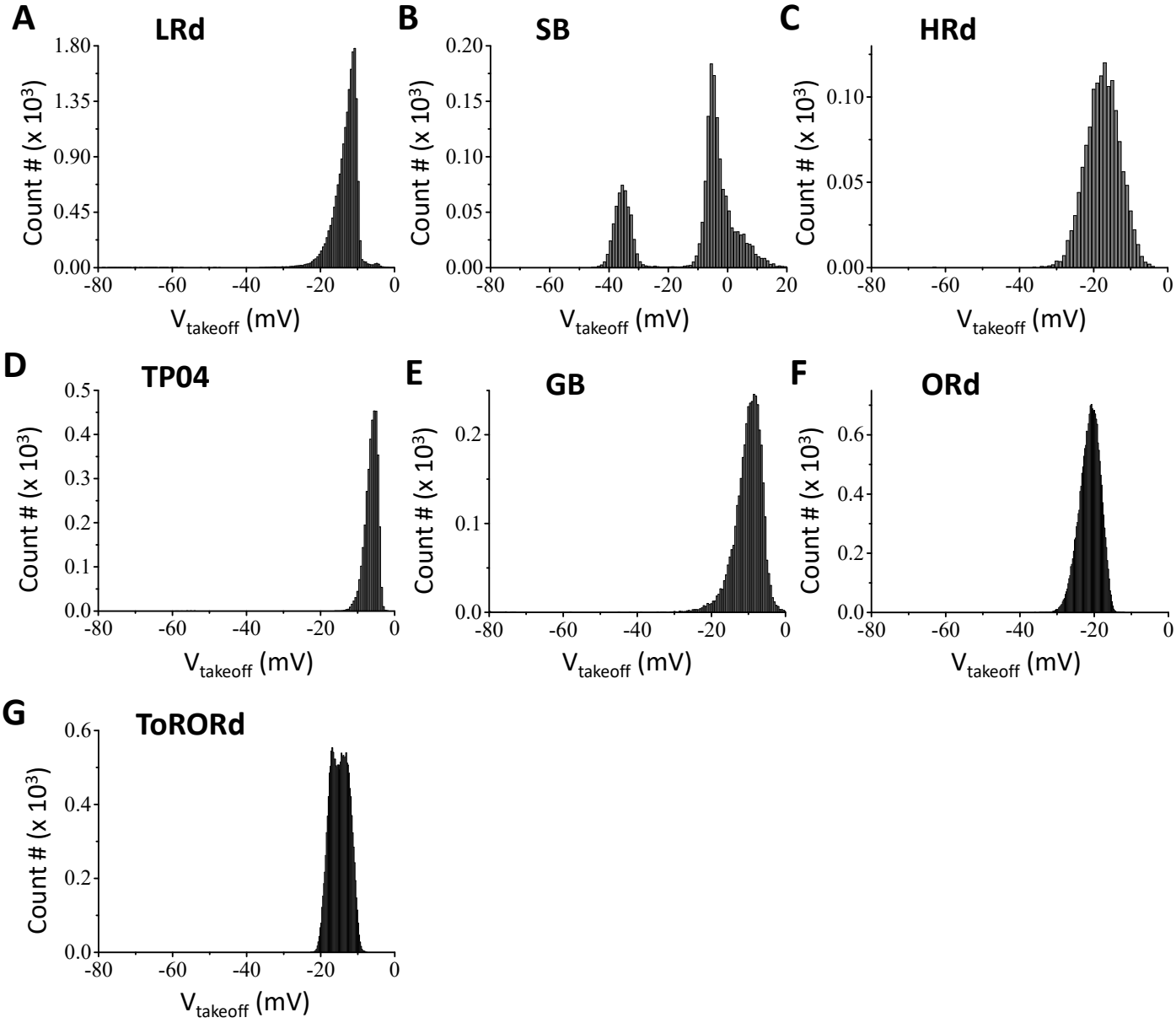

Figure S3. **Histograms of EAD take-off potentials**. The parameters were drawn randomly from pre-assigned intervals as described in Methods. **A**. LRd. **B**. SB. **C**. HRd. **D**. TP04. **E**. GB. **F**. ORd. **G**. ToRORd.

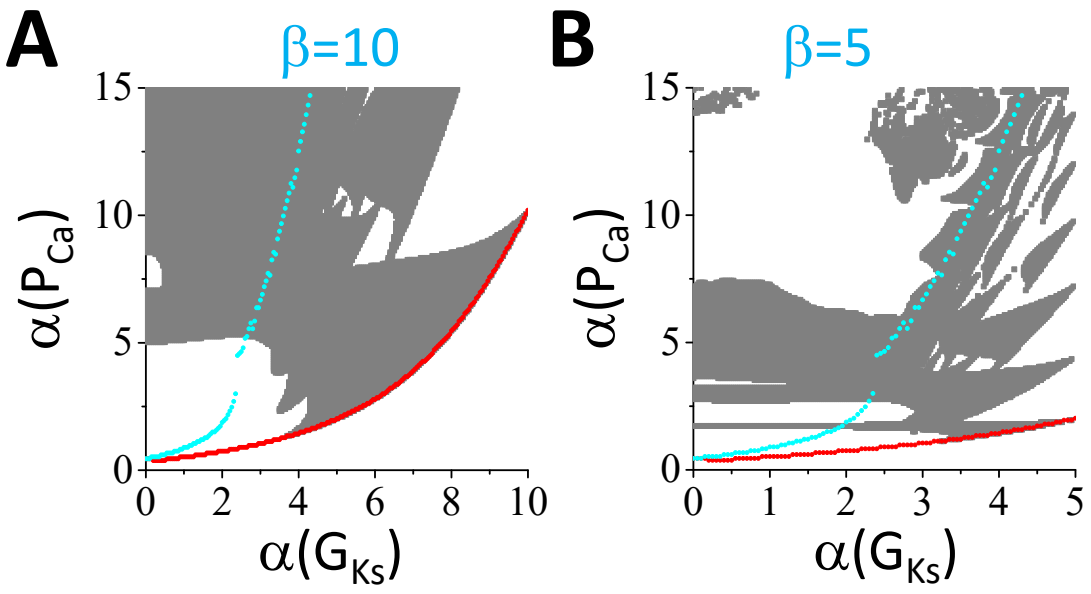

Figure S4. **Phase diagrams for the ORd model for two different β-values.** Panel **A** is the same replot of the LQT2 case in Fig.2F (β=10), replotted here for the purpose of comparison. Panel **B** is for β=5. Reducing β results in more bar and belt structures of phase diagram. Note that the PVCs still occur above the EAD boundaries which are identical in A and B. Therefore, β alters the phase diagram but does not alter the lower boundary of PVCs.

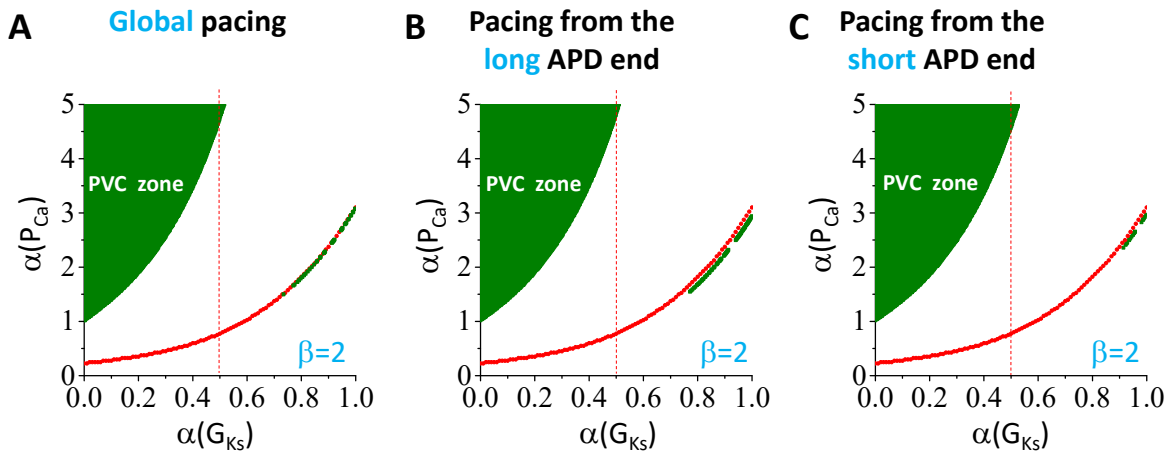

Figure S5. **Phase diagrams showing PVC regions under different pacing protocols for the LRd model under the condition of LQT2**. **A**. Phase diagram under global pacing, which is the same diagram shown in the middle panel of Fig.2A. **B**. Phase diagram under pacing from the long APD end of the cable. **C**. Phase diagram under pacing from the short APD end of the cable. The olive region or dots are where PVCs occur and the red dots are the lower EAD boundary of the single cell. The vertical dashed line in each panel is a reference line.

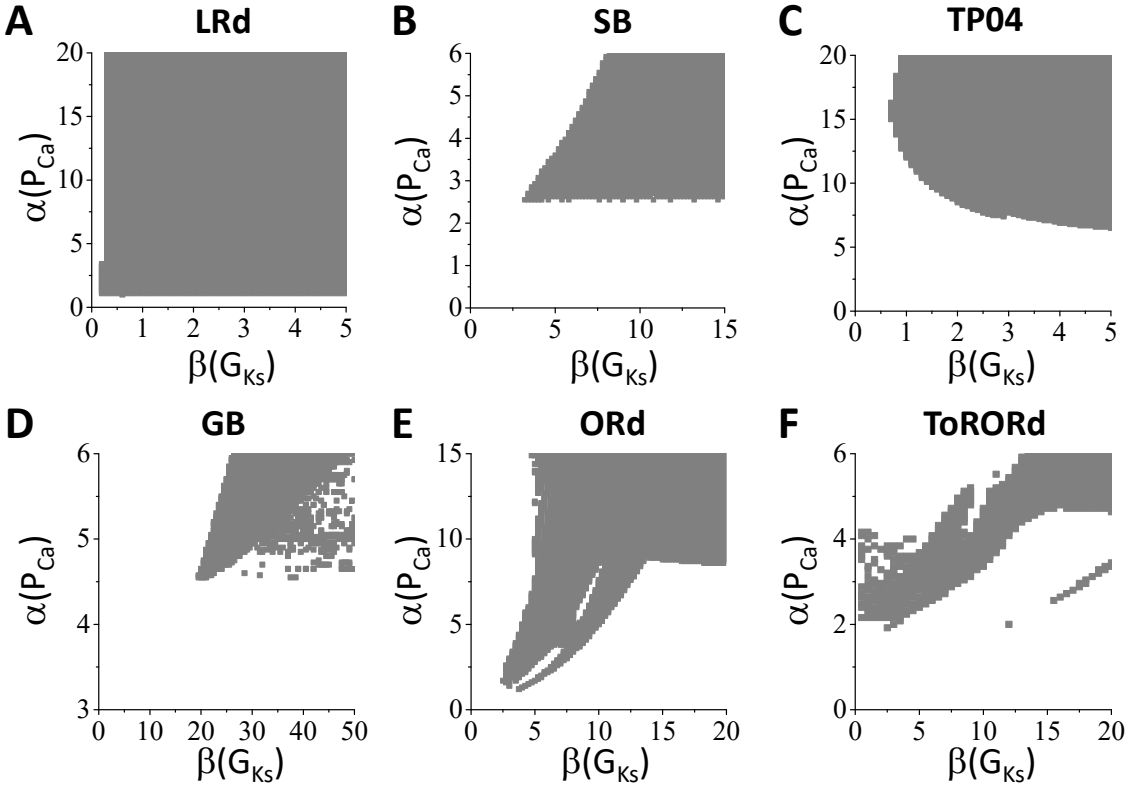

Figure S6. **Effects of increasing G_{Ks} in the short APD region on PVC genesis**. 1D cable simulations under the conditions of LQT2 for the 6 AP models. The same as Fig.5 in the main text except that $\alpha(G_{Ks}) = 0$.

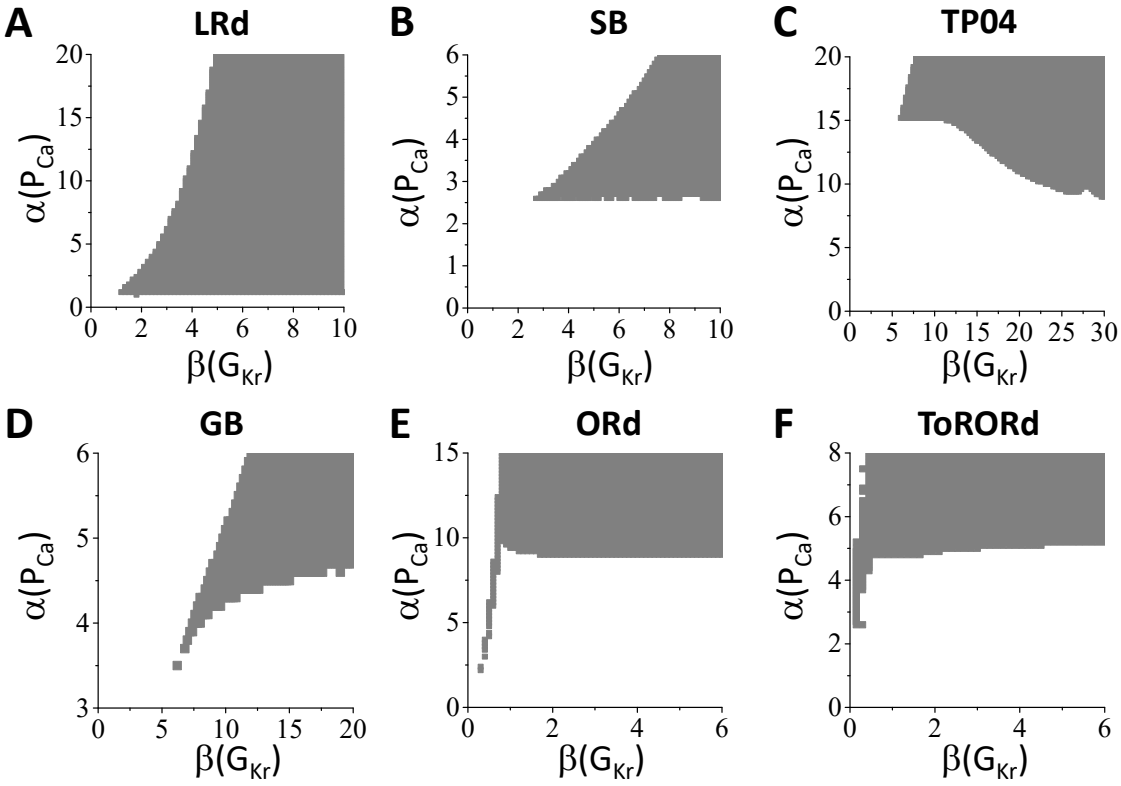

Figure S7. **Effects of increasing G_{Kr} in the short APD region on PVC genesis**. 1D cable simulations under the conditions of LQT1 for the 6 AP models. $\alpha(G_{Kr}) = 0$.

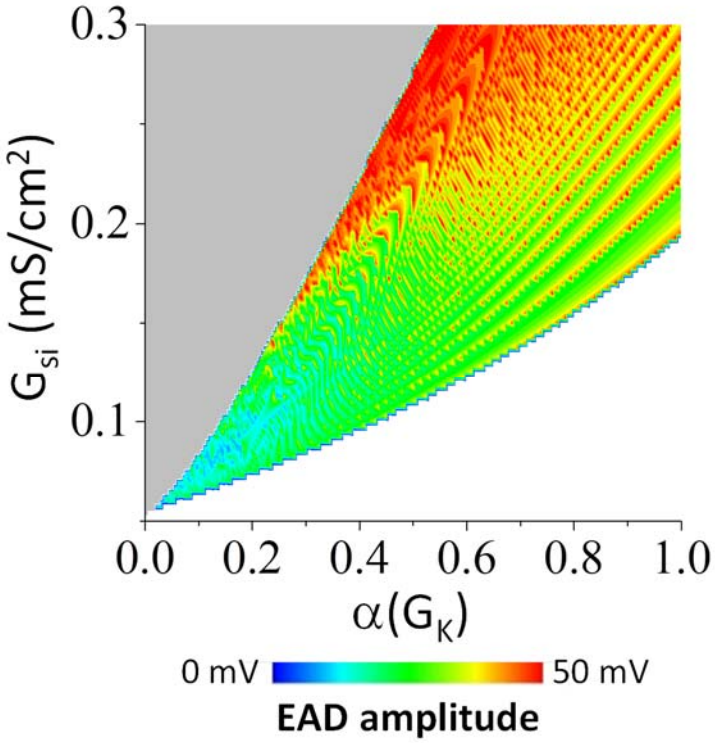

Figure S8. **EADs and repolarization failure in the LR1 model**. Shown are repolarization failure (gray) and EADs (color) for different G_{si} and $\alpha(G_K)$. The color scale indicates the amplitude of EADs.

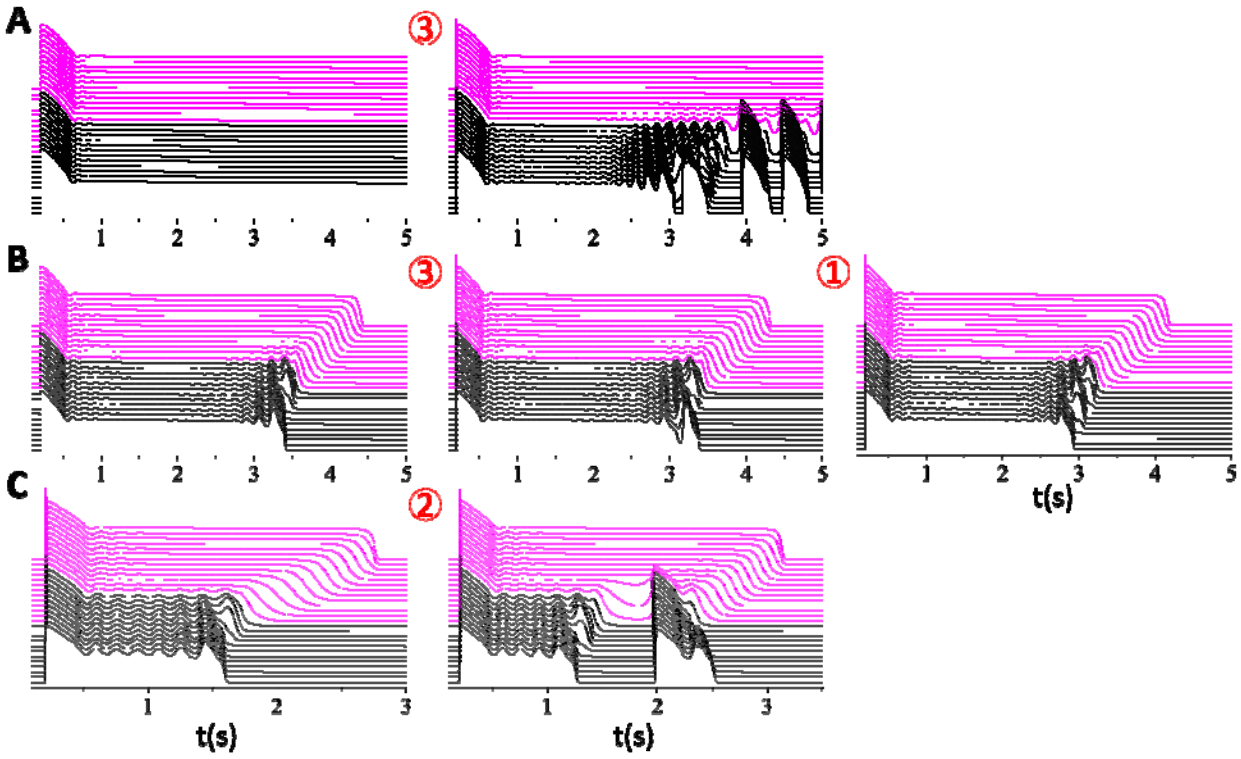

Figure S9. **Responses at the different boundaries of the phase diagram**. The numbers "1", "2", and "3" are boundaries labeled in Fig.10F. Shown are 3D plots (time-space-voltage) at both sides of the boundaries. **A**. Boundary "3". Left: repolarization fails in the whole cable. G_{si}=0.22 mS/cm^2 and $\alpha(G_K)$=0.48. Right (PVC region): Repolarization occurs in the short APD region, and an EAD-associated PVC and RG-induced PVCs occur. G_{si}=0.22 mS/cm^2 and $\alpha(G_K)$=0.52. **B**. Boundaries "3" and "1". Left: The RG is too mild to generate PVCs. G_{si}=0.17 mS/cm^2 and $\alpha(G_K)$=0.43. Middle (PVC region): The RG is just right for the occurrence of an EAD-induced PVC. G_{si}=0.17 mS/cm^2 and $\alpha(G_K)$=0.44. Right: The RG is too strong to generate PVCs. G_{si}=0.17 mS/cm^2 and $\alpha(G_K)$=0.45. **C**. Boundary "2". Left: both regions repolarize but the RG is not strong enough to promote PVCs. G_{si}=0.15 mS/cm^2 and $\alpha(G_K)$=0.55. Right (PVC region): The RG is large enough to result in an RG-induced PVC. G_{si}=0.15 mS/cm^2 and $\alpha(G_K)$=0.56.

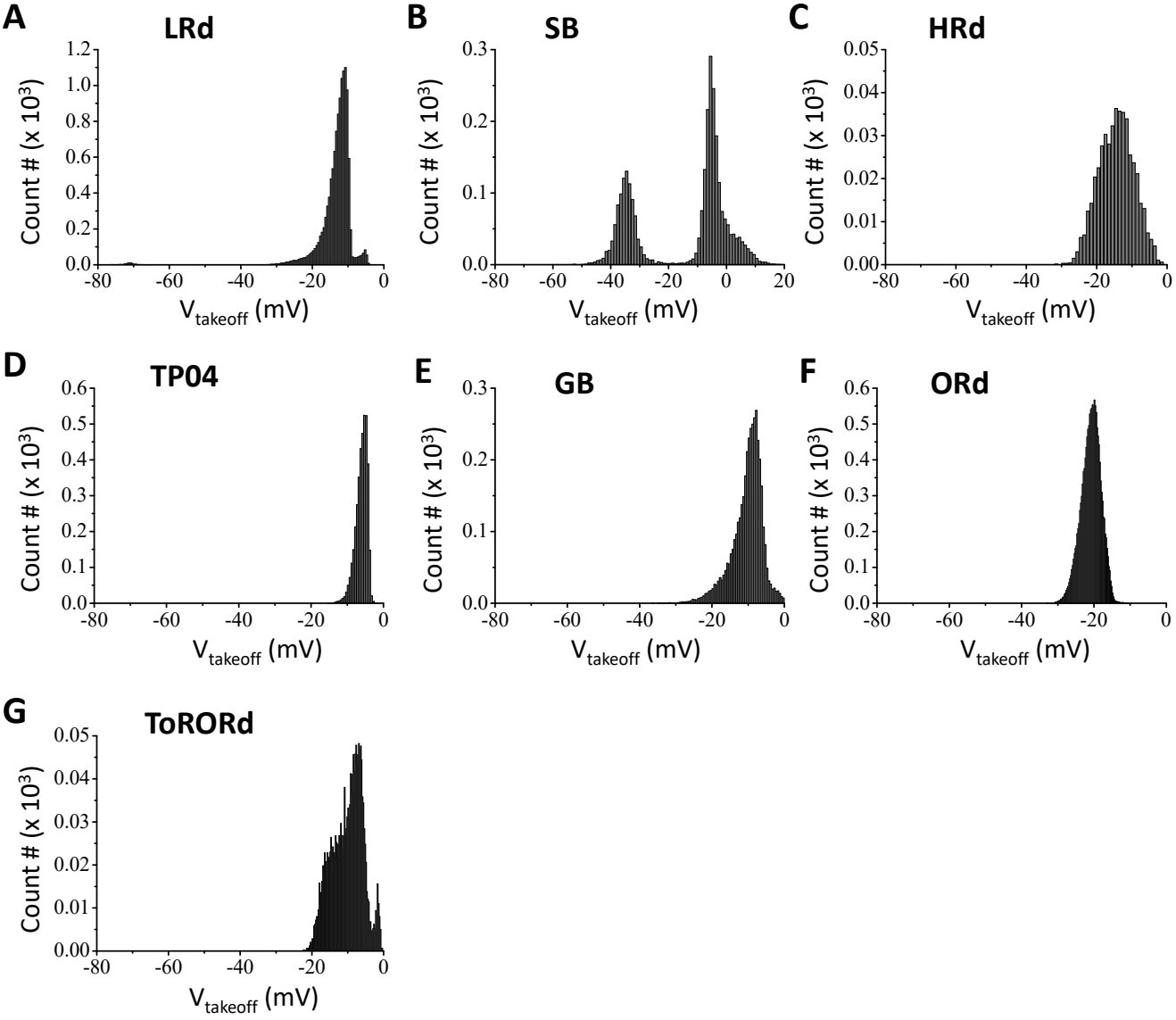

Figure S10. **Histograms of EAD take-off potentials with SERCA activity being 3 times the control value**. The parameters were drawn randomly from pre-assigned intervals as described in Methods, which were the same as SI Fig.S3 except that the SERCA activity of each model was 3 times of the control value. Comparing with SI Fig.S3, tripling the SERCA activity only had a small effect on the takeoff potential distributions. **A**. LRd. **B**. SB. **C**. HRd. **D**. TP04. **E**. GB. **F**. ORd. **G**. ToRORd.